HHS Public Access

Author manuscript

Cancer Res. Author manuscript; available in PMC 2024 May 15.

Published in final edited form as:

Cancer Res. 2023 November 15; 83(22): 3726–3738. doi:10.1158/0008-5472.CAN-23-0783.

Galectin-3 Cooperates with CD47 to Suppress Phagocytosis and T cell Immunity in Gastric Cancer Peritoneal Metastases

Yibo Fan[1], **Shumei Song**[1,*], **Yuan Li**[1,#], **Shilpa S Dhar**[2], **Jiankang Jin**[1], **Katsuhiro Yoshimura**[1], **Xiaodan Yao**[1], **Ruiping Wang**[3], **Ailing W Scott**[1], **Melissa Pool Pizzi**[1], **Jingjing Wu**[1], **Lang Ma**[1], **George A. Calin**[5], **Samir Hanash**[4], **Linghua Wang**[3], **Michael Curran**[6], **Jaffer A. Ajani**[1,*]

[1]Department of Gastrointestinal Medical Oncology, The University of Texas MD Anderson Cancer Center, Houston, TX 77030, USA.

[2]Department of Molecular and cellular Oncology, The University of Texas MD Anderson Cancer Center, Houston, TX 77030, USA.

[3]Department of Genomic Medicine, The University of Texas MD Anderson Cancer Center, Houston, TX 77030, USA.

[4]Department of Clinical Cancer Prevention, The University of Texas MD Anderson Cancer Center, Houston, TX 77030, USA.

[5]Department of Translational Molecular Pathology, The University of Texas MD Anderson Cancer Center, Houston, TX 77030, USA.

[6]Department of Immunology, The University of Texas MD Anderson Cancer Center, Houston, TX 77030, USA.

Abstract

The peritoneal cavity is a common site of gastric adenocarcinoma (GAC) metastasis. Peritoneal carcinomatosis (PC) is resistant to current therapies and confer poor prognosis, highlighting the need to identify new therapeutic targets. CD47 conveys a “don’t eat me” signal to myeloid cells upon binding its receptor SIRPα, which helps tumor cells circumvent macrophage phagocytosis and evade innate immune responses. Previous studies demonstrated that the blockade of CD47 alone results in limited clinical benefits, suggesting that other target(s) might need to be inhibited simultaneously with CD47 to elicit a strong anti-tumor response. Here, we found that CD47 was highly expressed on malignant PC cells, and elevated CD47 was associated with poor prognosis. Galectin-3 (Gal-3) expression correlated with CD47 expression, and co-expression of Gal-3 and

[*]**Correspondence**: Shumei Song, MD, Ph.D, Tel: +1-713-834-6144, ssong@mdanderson.org; Jaffer A. Ajani, MD, Tel: +1-713-792-2828, jajani@mdanderson.org, Department of Gastrointestinal Medical Oncology, The University of Texas MD Anderson Cancer Center, 1515 Holcombe Blvd., Houston, TX 77030, USA.

[#]Current address: Department of Surgical Oncology and General Surgery, First Hospital of China Medical University, Shenyang, 110001, P.R. China.

Author contributions

Conceptualization: SS, JA, Methodology: YF, YL, SD, JJ, XY, RW, AS, MP, KY, LM, GC, SH, LW, Investigation: YF, XY, JW, Visualization: YF, SS, JA, LW, MC, Funding acquisition: SS, JA, Project administration: SS, JA, Supervision: SS, JA, Writing –original draft: YF, SS, JA, Writing – review & editing: YF, SS, JA

Conflict interests:

The authors confirm that there are no conflicts of interest to disclose.

CD47 was significantly associated with diffuse type, poor differentiation, and tumor relapse. Depletion of Gal-3 reduced expression of CD47 through inhibition of c-Myc binding to the CD47 promoter. Furthermore, injection of Gal-3 deficient tumor cells into either wild-type and Lgals3−/− mice led to a reduction in M2 macrophages and increased T cell responses compared to Gal-3 wild-type tumor cells, indicating that tumor cell-derived Gal-3 plays a more important role in GAC progression and phagocytosis than host-derived Gal-3. Dual blockade of Gal-3 and CD47 collaboratively suppressed tumor growth, increased phagocytosis, repolarized macrophages, and boosted T cell immune responses. This data uncovered that Gal-3 functions together with CD47 to suppress phagocytosis and orchestrate immunosuppression in GAC with PC, which supports exploring a novel combination therapy targeting Gal-3 and CD47.

Keywords

CD47; Galectin-3; Phagocytosis; Peritoneal metastasis; Gastric adenocarcinoma

Introduction

Gastric adenocarcinoma (GAC) imposes a significant global health burden and is frequently diagnosed in an advanced stage with peritoneal carcinomatosis (PC), a frequent type of metastasis. Patients with PC have a short overall survival (less than 6 months), overwhelming symptoms, but limited ineffective or transiently palliative treatments(1–3). Immunotherapies that inhibit immune checkpoints (i.e., PD-1 or CTLA-4, etc.) have modestly improved patient outcomes in untreated metastatic and refractory cancer types. By integration large-scale GAC datasets including TCGA STAD and GSE15459, we found that Cluster of Differentiation 47 (CD47) expression is extremely high in GAC. The innate immune signaling can facilitate recognition and clearance of malignant cells through phagocytosis but also plays a key role in tumor-mediated immune escape(4–7). CD47 protein, expressed on both healthy and cancer cells, plays a pivotal role as an innate immune checkpoint by conveying a “don’t eat me message” upon binding to the signal-regulatory protein alpha (SIRPα) receptor on the myeloid cells(8) and prevents macrophage phagocytosis. Preclinical and early clinical data have suggested the promise of targeting phagocytosis checkpoints, such as the CD47 and SIRPα axis, either alone or in combination with established therapies (9–13). It has been reported that CD47 expression is associated with poor prognosis and blocking CD47 on GAC cells can provide an advantage in the preclinical setting(14). However, the potential value of CD47 as a therapeutic target in GAC patients with PC remains unclear.

Galactin-3 (Gal-3) regulates expression of a multitude of gene products involved in cell proliferation, growth, self-renewal, differentiation, and apoptosis(15,16). Overexpression of Gal-3 in tumors has been implicated in cancer progression and metastases(15,17,18). Additionally, Gal-3 plays a crucial role in promoting tumor-driven immune suppression. Gal-3 can bind to the T cell receptor (TCR) as a component of the synapse on cell surface, thereby restricting TCR movement, potentiating TCR down-regulation, and suppressing early activation of T cells through the TCR signaling pathway(19). Gal-3 deficient mice exhibit improved $CD8^+$ T cell effector function. Gal-3 can suppress CD8 T cell function by

binding to LAG3 in T cells and also increases IFNγ and Granzyme B production(19). Gal-3 expression on both tumor cells and host-derived cells within the tumor microenvironment (TME) mediates T-cell suppression(20). Studies have also reported that inhibition of tumor-derived Gal-3 led to the expansion of tumor-reactive T cells in *vitro*(21). Furthermore, tumor-derived Gal-3 alters macrophage polarization from M1 to M2 thus facilitating immune evasion(22). However, it is still unknown whether Gal-3 collaborates with CD47 to regulate the innate and T cell immunity for novel therapeutic strategy against GAC.

In this study, using bulk RNA-seq and two independent datasets of scRNA-seq, immunohistochemistry, and immunofluorescent staining of PC specimens and serial functional studies, syngeneic mouse model and *Lgals3*−/− mice, we uncovered that CD47 was highly expressed on PC cells and associated with a poor prognosis. We further demonstrated that CD47 and Gal-3 were highly co-expressed in PC cells and Gal3/CD47 high was frequent highly expressed in diffuse type and tumor relapses. Mechanistically, depletion of Gal-3 in GAC cells reduced expression of CD47 through inhibition of c-Myc binding to the CD47 promoter. Further, Gal-3 KO in GAC cells resulted in a reduction in M2 macrophages and increased T cell responses. Inhibition Gal-3 amplified consequences of inhibition of CD47 by increasing macrophage phagocytosis of GAC cells and T cell infiltration *in vitro* and *in vivo*. Our results suggested that dual inhibition of Gal-3 and CD47 could produce maximum benefit against GAC PC and could be a promising therapeutic strategy against PC.

Materials and Methods

Cells and reagents

The human gastric cancer cell lines AGS (RRID: CVCL_0139), GT5 (RRID: CVCL_8114) were purchased from American Type Culture Collection. KP-Luc2 murine GAC cell line was from Dr. Jo Ishizawa in the Department of Leukemia of MDACC and was previously reported(23). All cell lines have been profiled, authenticated and *Mycoplasma* testing, in the Cell Line Core Facility at The University of Texas MD Anderson Cancer Center, every 6 months. TD139 was from Selleck Chem (Cat#S0471) and neutralizing CD47 antibody was from Bio X Cell (Cat# BEO270).

Patient cohort of PC

PC specimens were collected at The University of Texas MD Anderson Cancer Center (Houston, USA) under an Institutional Review Board-approved protocol (no. LAB01–543) after obtaining written, informed consent from each participant. Patients with diagnosed GAC-PC with ascites were approached when they required a therapeutic paracentesis. No other selection criteria were applied. This project was in accordance with the policy advanced by the Helsinki Declaration of 1964 and later versions.

Phagocytosis assay

For *in vitro* phagocytosis assay by flow cytometry, 5×10^4 macrophages were plated per well in a 24 well tissue-culture plate. Cells from cell lines that lack endogenous fluorescence —AGS NC and Gal-3 KO cell were fluorescently labelled with CellTracker™ Green

CMFDA Dye (Thermo Fisher Scientific, Cat#C7025) per the manufacturer's instructions for 30 min at 37 °C and washed twice with 40 ml PBS before co-culture. Macrophages were incubated in serum-free medium for 2 h before adding 2×10^5 tumor cells and then were fluorescently labelled with CellTracker™ Red CMTPX Dye (Thermo Fisher Scientific, Cat#C34552) per the manufacturer's instructions for 30 min at 37 °C and washed twice with 40 ml PBS before co-culture. The aCD47 antibodies (10 μg/mL) and TD139 (100 nM) were added into tumor cells 2 days before co-cultured with macrophage. After co-cultured 2 h at 37°, flow cytometry detected GFP^+ out of $F4/80^+$ cells. For in vivo phagocytosis was measured as the percentage of GFP^+ out of $F4/80^+$ TAMs. For in vitro phagocytosis assay by immunofluorescence, macrophage and tumor were incubated for 6 h in an incubator at 37 °C. After incubation, wells were washed vigorously two times with serum-free RPMI in order to wash away non-phagocytosed tumor cells, then visualized under the Nicon T2 confocal laser scanning microscope.

In vivo xenograft tumor-growth experiments

8 weeks old C57BL/6 and B6.Cg-*Lgals3*^{tm1Poi}/J (#006338, *Lgals3−/−)* mice were purchased from Jackson Laboratory and maintained at a pathogen-free facility at MD Anderson Cancer Center. KP-Luc2 NC and Gal-3 KO cells were subcutaneously injected into C57BL/6 and B6.Cg-*Lgals3*^{tm1Poi}/J, respectively. C57BL/6 mice were subcutaneously injected with 1×10^5 KP-Luc2 cells per site. 5 days after tumor cells incubation, mice were randomly grouped to receive treatment with PBS, aCD47 antibody (intraperitoneal injection, 200μg/mouse, 2 times a week), TD139 (intraperitoneal injection, 300μg/mouse, 3 times a week). Mice with sum tumor volume >2000 mm^3, ulcer >5 mm, hypoactivity or hunched posture were euthanized. All animal experiment were performed in compliance with approved protocol (00001488-RN02) by the Institutional Animal Care and Use Committee at MD Anderson Cancer Center.

Statistical Analysis

Statistical analyses of flow cytometry and immunostaining quantifications were performed with one-way ANOVA with Tukey's multiple comparison test, unpaired, two-tailed t test, or Fisher's exact test using GraphPad Prism (GraphPad Software, San Diego, CA, USA). The expression levels of indicated genes among TCGA STAD cohort samples were based on the RNA Seq V2 RSEM data. TCGA data were downloaded from cBioPortal. For the survival analysis based on CD47 and CD274 expression, patients with available OS data and RNA-seq data (n = 415) were selected complete response (n=136), and then stratified into high (n = 68) and low (n = 68) groups based on the median expression level. Kaplan-Meier plots were drawn for survival analysis and the log rank Mantel-Cox test was used to evaluate statistical differences. RNA-sequencing data regarding expression levels for *SIRPA*, *PDCD1*, *LILRB1*, *LILRB2*, *CD47* and *CD274* from human tumors and matched healthy tissues collected by TCGA and GTEx were downloaded as log2(normalized counts +1) values from UCSC Xena27 (https://xenabrowser.net/). The expression of *CD47, SIPRA, CD274, PDCD1, CD28, EOMES, LAG3, ICOS, CTLA4, LILRB1, IDO1* was analyzed in Stage IV patients of TCGA STAD, GSE15459 and GSE62254. A P value < 0.05 was considered statistically significant. Error bars represented standard error of the mean (S.E.M.) when multiple visual fields were averaged to produce a single value for each

animal, which was then averaged again to represent the mean bar for the group in each graph.

Data and materials availability

All dataset and materials generated from this study are available for scientific community upon request. The data analyzed in this study are publicly available in TCGA Firehose STAD dataset and in the Gene Expression Omnibus (GEO) at accession numbers GSE15459 and GSE62254. RNA-Seq data have been deposited at the European Genome-phenome Archive (EGA). The datasets can be fully accessed under the accession number EGAS00001003180. All single-cell RNA-sequencing data generated by this study have been be deposited in the European Genome-Phenome Archive (EGA, https://ega-archive.org/). The data can be accessed under the accession number EGAS00001004443. Access can be granted by request from the corresponding author (Jaffer Ajani, jajani@mdanderson.org). All other raw data are available upon a reasonable request to the corresponding author.

Results

The CD47 “Don’t eat me” signal is enriched in human metastatic GAC

The “Don’t eat me” signal consists of several inhibitory receptors and their ligands on epithelial cells and myeloid cells including CD47/SIRPα, MHC1/LILRB1/LILRB2, and PD-L1/ PD-1 (Fig.S1A) which play a pivotal role in physiologic homeostasis of normal tissues. We systematically analyzed the transcriptome of immune checkpoints and “don’t eat me” genes in the bulk RNA-seq data from PC specimens and uncovered that *CD47* and *SIRPA* were highly enriched among other “don’t eat me” genes and immune checkpoints (Fig. 1A and Supplementary Table 1). Intriguingly, we observed *CD47* also highly expressed in two- GAC datasets of stage IV patients (Fig. 1B). Our scRNA-seq data in 20 PC specimens revealed that *CD47* and its receptor *SIRPA* were highly expressed in tumor cell cluster and myeloid cluster respectively (Fig.1C). Further, we validated the immune and epithelial markers by CyTOF in PC specimens and also observed that CD47 was highly expressed in cytokeratin positive tumor cell clusters, whereas PD-L1 expression was hardly detected in most cells (Fig. 1D). More importantly, we observed that increased expression of *CD47* in patients with short-term survivors (Fig. 1E–F). To further elucidate CD47 expression in different cell types in the PC specimens, we performed flow cytometry in PC cells from 42 cases (Fig. S1B and Supplementary Tables 2). Further analyses revealed that high expression of CD47 in $EpCAM^+$ tumor cells was significantly associated with shorter survival (Fig.1G). Finally, we observed that high expression of CD47 was significantly associated with shorter survival and disease-free survival even in the complete responder (CR) group of TCGA STAD cohort (Fig. 1H and Fig. S1C) which prompted us to focus on CD47 in rest of the study. Altogether, these data suggested that CD47 was highly expressed in PC cells and prognosticates shorter survival in GAC patients with PC.

Gal-3 correlated with CD47 expression in both primary and metastatic GAC

We previously reported that Gal-3 was an independent prognosticator of shorter survival and potentially a novel therapeutic target particularly in diffuse type GAC(24). scRNA-seq of 20 PC specimens identified that *LGALS3* was one of the top genes and highly expressed

in 13 tumor cell clusters (Fig. 2A and Supplementary Table 3). Further scRNA-seq analysis revealed that *LGALS3* positively correlated with *CD47* in tumor cell clusters of shorter survivors (Fig. 2B and Fig. S2A–B). The positive correlation between Gal-3 and CD47 was also observed in epithelium cell cluster of PC samples in another independent cohort (25) (Fig. 2C). To further validate the correlation of expression between CD47 and Gal-3 in PC specimens, we stained 51 PC samples (Supplementary Table 4) and found that the expression of CD47 was significantly positive associated with expression of Gal-3 (Fig. 2D), and we also found that CD47 and Gal-3 frequently co-expressed on the paired primary tumor and ascites samples (Fig. S2C–D). Furthermore, we validated the expression of Gal-3 and CD47 by immunohistochemistry staining in a primary GAC TMA containing 210 patients and found that the expression of CD47 and Gal-3 was increased in both intestinal and diffuse GAC tissues compared to non-tumor tissues and the expression of CD47 was positively associated with the expression of Gal-3 in primary tumor tissues (Fig. 2E and Supplementary Table 5). Most importantly, we found that high expression of both CD47 and Gal-3 was significantly associated with shorter survival (Fig. 2F), poorly differentiated GAC, diffuse type, and a higher rate of relapse compared to low expression (Fig. 2G). Together, we note that CD47 and Gal-3 were positively correlated in both primary and PC samples.

Down-regulation of Gal-3 suppressed CD47 expression in GAC cells

Having observed that CD47 was highly expressed in primary and metastatic GAC, we note that fewer studies have focused on the parameters that regulate CD47 and its related “don’t eat me” signaling. Previous studies have shown that cytokines including TNFα, IL6, and IFN-γ are involved in regulating CD47 expression(26,27). c-Myc and HER2 were reported oncogenes that regulated CD47 expression in tumors(11,28). Based on the finding that Gal-3 was positively associated with CD47 in the primary and metastatic GAC tissues, we sought to explore if the potential regulation of Gal-3 on CD47 in in GAC cells. First, we generated Gal-3 KO in GAC cell lines AGS and GT5 using Lenti-CRISPR/Cas9 and validated successful KO of Gal-3 in AGS and GT5 by western blot. Interestingly, we found that Gal-3 KO decreased CD47 expression at the protein level (Fig. 3A) and significantly decreased CD47 mRNA expression in both GAC cell lines (Fig. 3B). Furthermore, down-regulation of Gal-3 decreased CD47 expression by flow cytometry in both AGS and GT5 GAC cell lines (Fig. 3C–D). To further validate this finding, we co-stained CD47 and Gal-3 in Gal-3 KO GAC cells compared to control (NC) cells of AGS and GT5 and found that CD47 expression was dramatically decreased upon Gal-3 KO in two individual clones in AGS and GT5 cell (Fig. S3A). To further elucidate the mechanisms by which Gal-3 regulates CD47, we performed RNAseq in AGS cells with Gal-3 KO vs NC cells, and GSEA analysis revealed that MYC-Targets V1 and MYC-Targets V2 signaling were significantly decreased upon Gal-3 KO (Fig. 3E–F and Fig. S3B). Gal-3 KO reduced c-Myc expression was further validated by western blot in both human AGS cell line and mouse KP-Luc2 cell lines (Fig. S3C) which in line with our prior study demonstrated that overexpression of Gal-3 increased c-Myc expression in SNU1 with non-Gal-3 GAC cell line(24). Additionally, our previous study and those by others have demonstrated that Gal-3 regulates c-Myc and activates Wnt signaling through binding to β-catenin and TCF4 (17,29,30). In the present study, we also confirmed that Gal-3 KO dramatically decreased the β-catenin and c-Myc levels, while

re-expression of Gal-3 in Gal-3 KO cells increased the β-catenin and c-Myc levels indicating Gal-3 regulation of β-catenin and c-Myc in GAC cells (Fig. S3D). To elucidate the role of c-Myc in regulating CD47 downstream of Gal-3, we conducted siRNA-mediated c-Myc knockdown in AGS cells and found that c-Myc knockdown reduced CD47 expression, but Gal-3 expression had no significant impact compared with Scramble-treated cells (Fig. S3E). Furthermore, a recent study has demonstrated that c-Myc regulates CD47 through binding directly to the promoter of CD47 in human and murine leukemia and lymphomas to regulate CD47 transcription (28,31). Thus, we hypothesize that Gal-3 regulates CD47 through transcriptional factor c-Myc. To prove this, we analyzed ChIP seq data in multiple cancer cell datasets pulling down chromatin by c-Myc antibody and found that CD47 locus was enriched in three ChIP seq datasets (Fig. S4A). We performed ChIP-qPCR after c-Myc pulldown chromatin in Gal-3 KO cells compared to NC and noticed that KO Gal-3 significantly decreased c-Myc occupancy in the promoter of CD47 using specific CD47 primers spanning c-Myc binding site of the CD47 promoter. Correspondingly, occupancy of the chromatin open and activation marker, H3k27ac in CD47 promoter was dramatically reduced upon Gal-3 KO in GAC cell line (Fig. S4B–C). To further confirm the role of c-Myc in the regulation of CD47 by Gal-3, we conducted c-Myc overexpression in Gal-3 KO cells and found that CD47 expression was enhanced in cells rescued c-Myc (Fig. 3G). Further, we performed ChIP-qPCR using c-Myc antibody pulldown chromatin at two c-Myc binding sites of CD47 promoter (Fig.S4B) and found that c-Myc and H3k27ac occupancy in the promoter of CD47 were decreased in Gal-3 KO cells and were reversed by Gal-3 overexpression (Fig. 3H and Fig.S4C) suggesting Gal-3 regulation of CD47 in GAC cells required c-Myc occupancy of the CD47 promoter. Besides, we conducted Gal-1 and Gal-2 overexpression in AGS cells and confirmed by qRT-PCR (Fig. S4D) and detected levels of c-Myc, CD47, and Gal-3 expression by Western blot. No obvious changes in the levels of c-Myc and CD47 upon Gal-1 and Gal-2 overexpression compared with NC cells (Fig. S4E), suggesting that neither Gal-1 nor Gal-2 had an impact on CD47 and c-Myc expression.

Depletion of Gal-3 in tumor cells promotes phagocytosis by repolarized macrophages

To elucidate the effects of tumor cell-derived Gal-3 or host Gal-3 on innate immune response, we utilized our *Lgals3*−/− vs WT mice and inoculated murine KP-Luc2 tumor cells with NC or Gal-3 KO into WT mice and *Lgals3*−/− mice respectively (Fig. 4A, left). As a result, we noticed that KO Gal-3 in KP-Luc2 tumor cells significantly reduced tumor growth and increased phagocytosis of F4/80 on tumor cells (GFP^+) in both WT and *Lgal3*−/− mice, although Gal-3 KO in KP-Luc2 tumor cells demonstrated better antitumor effects in *Lgal3*−/− mice compared to WT mice ($P<0.0001$, Fig. 4A–B) indicating that tumor cell-derived Gal-3 plays more important role in GAC progression and phagocytosis than that of host-derived Gal-3. To further explore the impact of Gal-3 from GAC cells on macrophage repolarization and function, we co-cultured human macrophages derived from PBMCs with AGS NC and Gal-3 KO cells for 48 hours, and then the notable Mφ2 and Mφ1 marker were examined by qRT-PCR. M1-like macrophages related *CD80*, *CD86*, *TNFA,* and *CXCL10* were significantly increased when co-cultured with Gal-3 KO cells compared to untreated NC cells, whereas *TGFB1* and *TGFB2* were significantly reduced in human macrophages when co-cultured with Gal-3 KO AGS cells compared to NC cells (Fig. 4C). Similarly, U937 monocytes were co-cultured with AGS Gal-3 KO cells significantly

reduced the production of *CSF1, CCL2,* and *IL10* compared to that of AGS NC cells, indicating Gal-3 levels in GAC cells govern the macrophage function (Fig. 4D–E). To further explore the potential mechanisms that Gal-3 regulated macrophage polarization, we next examined GSEA analysis between NC and Gal-3 KO of AGS cells. We observed that the interferon alpha and interferon gamma response pathways were upregulated in Gal-3 KO cell compared with NC cells (Fig. S5A). This observation is in line with the previously study that both Type I and Type II interferons activate antitumor M1 macrophage (32–36). No significance of increase phagocytosis was observed in CD47 overexpression cells (Fig. S5B–C). Next, to elucidate the cooperative actions of Gal-3 and CD47 on phagocytosis of macrophage, bone marrow derived macrophages (BMDMs) were isolated from mice (Fig. 4F and Fig. S5D) and then BMDMs co-cultured with KP-Luc2 murine GAC cells pretreated with Gal-3 inhibitor TD139 or neutralizing CD47 antibody (αCD47) alone or combination treatment. As a result, the combination inhibition of Gal-3 and CD47 in KP-Luc2 cells led to significantly enhanced phagocytosis of BMDMs on KP-Luc2 cells when co-culture them *in vitro* (Fig. 4G and Fig. S5E). These results suggest that Gal-3 in either human GAC cells or murine KP-Luc2 tumor cells is responsible to repolarize into M2 macrophages and suppresses macrophage phagocytosis and cooperates with CD47 protected GAC cells from phagocytosis.

Gal-3 prevents recruitment and activation of immune effector cells in GAC

To assess the role of Gal-3 in regulating adaptive T cell immune responses and the potential cooperation with CD47, we first examined CD8 T cell infiltration and response in KP-Luc2 tumors with or without Gal-3 KO in WT and *Lgals3−/−* mice. $CD8^+$ T cell infiltration in KP-Luc2 Gal-3 KO cell implanted GAC tumors significantly increased compared to that of the KP-Luc2 NC cells in WT mice and the $CD8^+$ T cell infiltration was even further boosted when KP-Luc2 Gal-3 KO tumor cells implanted into *Lgals3−/−* mice (Fig. 5A) indicating Gal-3 in both tumor cells and host plays an important role in limiting T cell infiltration. To further examine the association of Gal-3 with $CD8^+$ T cell, $CD4^+$ T cell, B cell, and NK cell infiltration, we explored TCGA GAC dataset by MCP-counter, xCELL and quanTIseq algorithms and found that the expression of Gal-3 were negatively correlated with $CD8^+$ T cell infiltration in all algorithms (Fig. 5B), which was consistent with the previous report that Gal-3 inhibitor GB1107 increased $CD8^+$ but not $CD4^+$ T cells within the tumor(22). To further explore the potential mechanisms that Gal-3 regulated T cell responses, we performed GSEA analysis between NC and Gal-3 KO of AGS cells and revealed that TNFa signaling via the NFKB pathway were upregulated in Gal-3 KO cell compared with NC cells (Fig.5C). In order to validate the effect of Gal-3 on T cell responses in GAC, we purified $CD8^+$ T cells from human PBMCs and co-cultured with AGS and GT5 NC and Gal-3 KO cells and then analyzed T cell responses using qRT-PCR and Flow-cytometry (Fig. S6A). The expression of *TNF, IL2,* and *IFNG* in PBMCs significantly increased in co-cultured with AGS Gal-3 KO cells compared to that in NC cells of AGS cells (Fig. 5D). We found that Granzyme B^+CD8^+ T cells and $Perforin^+CD8^+$ T cells in PBMCs were significantly increased in co-culturing with Gal-3 KO cells in both AGS and GT5 cells compared to NC cells (Fig. 5E–F). No significance change in the cytotoxic function of $CD8^+$ T cells was observed in CD47 overexpression cells (Fig. S6B–C). To elucidate whether there is cooperation between Gal-3 and CD47 on T cell responses, we treated

AGS cells with Gal-3 inhibitor TD139, neutralizing CD47 antibody (αCD47), and their combination for 2 days and co-cultured with human PBMCs for additional 2 days, then analyzed GrB and perforin production from $CD8^+$ T cells in PBMCs by flow cytometry. As a result, we found that tumor cells pretreated with the combination of TD139 and CD47 antibody significantly boosted T cell responses (Fig. 5G) in PBMCs compared to either alone, suggesting that inhibition Gal-3 has synergistic effects with anti-CD47 in activating cytotoxic T cell functions in GAC.

Inhibition Gal-3 synergized with CD47 blockage suppressed tumor progression in the syngeneic mouse model

Due to the high expression of Gal-3 and CD47 in metastatic GAC, their positive correlation and their regulation in innate and T cell immunity, we sought to investigate if targeting both Gal-3 and CD47 on innate and T cell immune responses could be recapitulated *in vivo.* For this, we first implanted KP-Luc2 murine GAC cells with labeled GFP luciferase into C57BL/6 mice, and then treated with TD139, αCD47 and combinational treatment (Fig. 6A and Fig. S7A). Tumor growth was monitored by bioluminescence weekly. At the end, tumors were collected, weighed, snap frozen or formalin-fixed and paraffin embedded for molecular analyses by qRT-PCR and IF staining for macrophage/T cells (F4/80 and CD8), and flowcytometry for T cell responses. As a results, the combinational treatment led to a robust reduction in tumor growth compared with the untreated or single treatment group (Fig. 6A and Fig. S7B). Correspondingly, we found increased phagocytosis in the combination group (Fig. 6B) and increased infiltration of F4/80 (Fig. S7C), which was in line with recent study(37) indicating that macrophages increased in the tumor microenvironment. More interestingly, TD139 significantly increased $IFN\gamma^+$ production by $CD8^+$ cells and cytotoxic T cell infiltration which further augmented when combining with CD47 blockage (Fig. 6C–D). More importantly, combination treatment increased the notable M1 macrophage markers-*Irf1, Irf5, Cd80, Cd86* expression, whereas decreased notable M2 macrophage markers-*Mrc1* and *Arg1* in the tumor microenvironment (Fig. 6E). Additionally, combination treatment significantly increased T cell response genes *Tnfa, Gzmb and Ifng* expression, indicating that the combination treatment repolarized macrophage and increased T cell infiltration as well as their cytotoxic function. Taken together, these data demonstrated that inhibition of Gal-3 synergized with CD47 blockade to suppress tumor progression through activation of both innate and adaptive immune responses (Fig. 6F).

Discussion

CD47 is one of the major players in conveying the “don’t eat me” signal upon binding its receptor SIRPα on the myeloid cells. There is considerable interest in targeting CD47 in the oncology space, however, little has been known about its role in GAC patients with PC. Our multiple profiling in PC cells has shown that CD47 overexpression in primary tumors and PC cells which correlated with poor patient survival. Both CD47 and Gal-3 were positively correlated, and KO of Gal-3 significantly decreased CD47 expression in GAC cell lines. Combined inhibition of CD47 and Gal-3 further increased phagocytosis by macrophages and enhanced $CD8^+$ T cell function *in vitro* and *in vivo*. Our data suggest that Gal-3 and CD47

dual inhibition produced most beneficial effects against advanced GAC cells and targeting both Gal-3 and CD47 could be a promising therapeutic strategy against GAC with PC.

CD47 is a trans-membrane protein ubiquitously expressed on human cells but overexpressed on many types of tumor cells. Signaling through the CD47-SIRPα axis plays an important role in the homeostatic processes including erythrocytes, platelets, and hematopoietic stem cell maintenance(8). Tumor cells upregulate CD47 that triggers an interaction between CD47 and SIRPα-the “don’t eat me” signaling in the macrophages, inhibiting phagocytosis to evade innate immune surveillance and to facilitate cancer growth and metastases(38). Thus, CD47-SIRPα blockade has emerged as a next-generation of cancer immunotherapies in various malignancies in the preclinical and clinical settings(39). Using scRNAseq and CyTOF as well as other methodologies, we discovered that CD47 is highly expressed in GAC tissues and PC cells which prompted us to target CD47 in GAC PC cells. However, several clinical studies suggest that blocking the CD47-SIRPα axis alone is not sufficient to induce tumor regression in several cancer types (9,40,41) which may be attributed by several aspects. 1). the phagocytosis relies on the balance between prophagocytic (eat me) in myeloid cells and antiphagocytic (don’t eat me) signals on targets cells(42). 2). CD47 levels are only modestly increased relative to surrounding healthy tissue in most human tumors(43). 3). The TME heterogeneity and co-exists with other innate and adaptive immune checkpoints such as B2M/LILRB1/2 or PD-1/PD-L1 etc. Thus, combination therapies are strongly recommended. Recent appealing data support the combination therapy of targeting of the CD47/SIRPα axis with other oncotargets or other immune checkpoint blockades to improved tumor control such as combination of anti-CD47 with trastuzumab, which eliminating HER2 positive breast cancer and overcomes trastuzumab resistance(44); combination with rituximab in lymphoma led to improved clinical responses(12). Combination with other immune checkpoint blockades such as CTLA-4i or PD-1i/PD-L1i has been studied by several research groups aiming to increase in the efficacy by blockade of the axes that cancer cells use to avoid being cleared by the immune system(45). In line with the present study that single treatment of αCD47 did not sufficiently influence phagocytosis and T cell responses in both in vivo and in vitro, few studies also indicated that combination treatment with αCD47 could be more efficient to suppress tumor growth (8,46). Thus far, only anti-PD-1 and Her2 antibodies have been approved by FDA in GAC. However, the expression of *PDCD1* and mutation/amplification of *ERBB2* was very low in our GAC specimens by whole exome sequencing (WES)(47), scRNA-seq, and CyTOF analysis which prompted us to explore other immune/oncotargets that highly expressed in GAC patients.

Several reports have noted that Gal-3 expression was significantly higher in poorly differentiated GAC and lymph node positive cancers(48–50). From our scRNA-seq data, we noticed that Gal-3 was the one of the top genes in tumor clusters and it positively correlated with CD47 in both primary and metastatic GAC. Intriguingly, we observed that the percentage of double positive cells was 45.04% in PC samples using scRNA-seq; and patients with double positive conferred worse prognosis. Most importantly, we found that Gal-3 positively regulated CD47 expression at the level of transcription through promoting c-Myc binding to the CD47 promoter in GAC. Further, we revealed that overexpression of c-Myc in AGS Gal-3 KO cells significantly increased CD47 expression indicating c-Myc

upregulated CD47 expression downstream of Gal-3, which is in line with previously report (28). Gal-3 has been reported mediating both innate and T cell immunosuppression thus forms an attractive target in addition to CD47. Tumor cells secrete Gal-3 that mediates innate and adaptive immune responses through promoting macrophage polarization from M1 to M2, inducing $CD8^+$ T cell apoptosis, and restricting TCR clustering(22). The compelling evidence of Gal-3 in boosting tumor growth and immune suppression has made it an exciting target for cancer therapy. The key finding in this study is that Gal-3 suppressed phagocytosis by macrophages and KO Gal-3 promoted phagocytosis and increased macrophage infiltration which in part through CD47 downregulation. Furthermore, we showed that phagocytosis significantly increased by macrophages when treated in TD139 especially in combination with anti-CD47 therapy. In the present study, blocking CD47 alone did not significantly induce T cell responses. However, when blocking CD47 in combination with inhibition of Gal-3 using TD139 significantly boosted phagocytosis and increased cytotoxic T cell function *in vitro*. Co-targeting Gal-3 and CD47 in the KP-Luc2 syngeneic mouse model, $CD8^+$ T cell infiltration, and T cell responses were synergistically increased along with tumor regression in *vivo*. Our studies have demonstrated that Gal-3 amplified CD47 signaling in innate immunity; and also have a direct effect to T cell immune responses. Taken together, these data demonstrated that inhibition of Gal-3 combined with CD47 blockade should be a strategy to follow.

In summary, our data uncovered that Gal-3 synergized with CD47 to suppress phagocytosis and orchestrated an immunosuppressed milieu in the tumor microenvironment. Dual blockade of Gal-3 and CD47 boosted both innate and adaptive T cell responses, thus providing rationale for a clinical trial in advanced GAC patients.

Supplementary Material

Refer to Web version on PubMed Central for supplementary material.

Acknowledgments

Public Health Service Grant DF56338 (SS), MD Anderson Institutional Research Grant 2021–00059328 (SS), Department of Defense grant CA210457, CA160433, CA170906, CA160445, CA200990, CA210439 (SS, JA), The National Institutes of Health grant CA269685, CA129906, CA138671, and CA172741 (SS, JA), Supported in part by the Caporella family, the Park family, the Dallas family, the Dio family, the Frankel family, the Kushner family, the Kohn family, the Smith family, Anonymous donor, the McNeil family, the Stupid Strong Foundation (Dallas, TX), and the Gastric Cancer Foundation (San Francisco, CA) (JA).

Abbreviations

GAC	gastric adenocarcinoma
PC	peritoneal carcinomatoses (implants or malignant ascites)
CD47	The Cluster of Differentiation 47
Gal3	Galectin-3
SIRPα	the signal-regulatory protein alpha

scRNA-seq	single-cell RNA-sequencing
RNA-seq	bulk RNA-sequencing
TME	the tumor microenvironment
CyTOF	Cytometry by time of flight
TMAs	tumor tissue microarrays
NC	normal control
qRT-PCR	quantitative real-time polymerase chain reaction
IHC	immunohistochemistry
IF	Immunofluorescence
Multi-IF	Multiplex-immunofluorescent staining
GrB	Granzyme B
CR	complete responder
αCD47	neutralizing CD47 antibody

References

1. Joshi SS, Badgwell BD. Current treatment and recent progress in gastric cancer. CA Cancer J Clin 2021;71:264–79 [PubMed: 33592120]
2. Chen D, Liu Z, Liu W, Fu M, Jiang W, Xu S, et al. Predicting postoperative peritoneal metastasis in gastric cancer with serosal invasion using a collagen nomogram. Nat Commun 2021;12:179 [PubMed: 33420057]
3. Tanaka Y, Chiwaki F, Kojima S, Kawazu M, Komatsu M, Ueno T, et al. Multi-omic profiling of peritoneal metastases in gastric cancer identifies molecular subtypes and therapeutic vulnerabilities. Nat Cancer 2021;2:962–77 [PubMed: 35121863]
4. Cassetta L, Pollard JW. Targeting macrophages: therapeutic approaches in cancer. Nat Rev Drug Discov 2018;17:887–904 [PubMed: 30361552]
5. Feng M, Jiang W, Kim BYS, Zhang CC, Fu YX, Weissman IL. Phagocytosis checkpoints as new targets for cancer immunotherapy. Nat Rev Cancer 2019;19:568–86 [PubMed: 31462760]
6. Isidori A, Cerchione C, Daver N, DiNardo C, Garcia-Manero G, Konopleva M, et al. Immunotherapy in Acute Myeloid Leukemia: Where We Stand. Front Oncol 2021;11:656218 [PubMed: 34041025]
7. Mantovani A, Marchesi F, Malesci A, Laghi L, Allavena P. Tumour-associated macrophages as treatment targets in oncology. Nat Rev Clin Oncol 2017;14:399–416 [PubMed: 28117416]
8. Logtenberg MEW, Scheeren FA, Schumacher TN. The CD47-SIRPalpha Immune Checkpoint. Immunity 2020;52:742–52 [PubMed: 32433947]
9. Ingram JR, Blomberg OS, Sockolosky JT, Ali L, Schmidt FI, Pishesha N, et al. Localized CD47 blockade enhances immunotherapy for murine melanoma. Proc Natl Acad Sci U S A 2017;114:10184–9 [PubMed: 28874561]
10. Ring NG, Herndler-Brandstetter D, Weiskopf K, Shan L, Volkmer JP, George BM, et al. Anti-SIRPalpha antibody immunotherapy enhances neutrophil and macrophage antitumor activity. Proc Natl Acad Sci U S A 2017;114:E10578–E85 [PubMed: 29158380]

11. Zhao XW, van Beek EM, Schornagel K, Van der Maaden H, Van Houdt M, Otten MA, et al. CD47-signal regulatory protein-alpha (SIRPalpha) interactions form a barrier for antibody-mediated tumor cell destruction. Proc Natl Acad Sci U S A 2011;108:18342–7 [PubMed: 22042861]
12. Advani R, Flinn I, Popplewell L, Forero A, Bartlett NL, Ghosh N, et al. CD47 Blockade by Hu5F9-G4 and Rituximab in Non-Hodgkin's Lymphoma. N Engl J Med 2018;379:1711–21 [PubMed: 30380386]
13. Sikic BI, Lakhani N, Patnaik A, Shah SA, Chandana SR, Rasco D, et al. First-in-Human, First-in-Class Phase I Trial of the Anti-CD47 Antibody Hu5F9-G4 in Patients With Advanced Cancers. J Clin Oncol 2019;37:946–53 [PubMed: 30811285]
14. Yoshida K, Tsujimoto H, Matsumura K, Kinoshita M, Takahata R, Matsumoto Y, et al. CD47 is an adverse prognostic factor and a therapeutic target in gastric cancer. Cancer Med 2015;4:1322–33 [PubMed: 26077800]
15. Song S, Byrd JC, Mazurek N, Liu K, Koo JS, Bresalier RS. Galectin-3 modulates MUC2 mucin expression in human colon cancer cells at the level of transcription via AP-1 activation. Gastroenterology 2005;129:1581–91 [PubMed: 16285957]
16. Braeuer RR, Zigler M, Kamiya T, Dobroff AS, Huang L, Choi W, et al. Galectin-3 contributes to melanoma growth and metastasis via regulation of NFAT1 and autotaxin. Cancer Res 2012;72:5757–66 [PubMed: 22986745]
17. Song S, Mazurek N, Liu C, Sun Y, Ding QQ, Liu K, et al. Galectin-3 mediates nuclear beta-catenin accumulation and Wnt signaling in human colon cancer cells by regulation of glycogen synthase kinase-3beta activity. Cancer Res 2009;69:1343–9 [PubMed: 19190323]
18. Zhao W, Ajani JA, Sushovan G, Ochi N, Hwang R, Hafley M, et al. Galectin-3 Mediates Tumor Cell-Stroma Interactions by Activating Pancreatic Stellate Cells to Produce Cytokines via Integrin Signaling. Gastroenterology 2018;154:1524–37 e6 [PubMed: 29274868]
19. Kouo T, Huang L, Pucsek AB, Cao M, Solt S, Armstrong T, et al. Galectin-3 Shapes Antitumor Immune Responses by Suppressing CD8+ T Cells via LAG-3 and Inhibiting Expansion of Plasmacytoid Dendritic Cells. Cancer Immunol Res 2015;3:412–23 [PubMed: 25691328]
20. Fermin Lee A, Chen HY, Wan L, Wu SY, Yu JS, Huang AC, et al. Galectin-3 modulates Th17 responses by regulating dendritic cell cytokines. Am J Pathol 2013;183:1209–22 [PubMed: 23916470]
21. Farhad M, Rolig AS, Redmond WL. The role of Galectin-3 in modulating tumor growth and immunosuppression within the tumor microenvironment. Oncoimmunology 2018;7:e1434467 [PubMed: 29872573]
22. Vuong L, Kouverianou E, Rooney CM, McHugh BJ, Howie SEM, Gregory CD, et al. An Orally Active Galectin-3 Antagonist Inhibits Lung Adenocarcinoma Growth and Augments Response to PD-L1 Blockade. Cancer Res 2019;79:1480–92 [PubMed: 30674531]
23. Okazaki S, Shintani S, Hirata Y, Suina K, Semba T, Yamasaki J, et al. Synthetic lethality of the ALDH3A1 inhibitor dyclonine and xCT inhibitors in glutathione deficiency-resistant cancer cells. Oncotarget 2018;9:33832–43 [PubMed: 30333913]
24. Ajani JA, Estrella JS, Chen Q, Correa AM, Ma L, Scott AW, et al. Galectin-3 expression is prognostic in diffuse type gastric adenocarcinoma, confers aggressive phenotype, and can be targeted by YAP1/BET inhibitors. Br J Cancer 2018;118:52–61 [PubMed: 29136404]
25. Kumar V, Ramnarayanan K, Sundar R, Padmanabhan N, Srivastava S, Koiwa M, et al. Single-Cell Atlas of Lineage States, Tumor Microenvironment, and Subtype-Specific Expression Programs in Gastric Cancer. Cancer Discov 2022;12:670–91 [PubMed: 34642171]
26. Johnson LDS, Banerjee S, Kruglov O, Viller NN, Horwitz SM, Lesokhin A, et al. Targeting CD47 in Sezary syndrome with SIRPalphaFc. Blood Adv 2019;3:1145–53 [PubMed: 30962222]
27. Kuriyama T, Takenaka K, Kohno K, Yamauchi T, Daitoku S, Yoshimoto G, et al. Engulfment of hematopoietic stem cells caused by down-regulation of CD47 is critical in the pathogenesis of hemophagocytic lymphohistiocytosis. Blood 2012;120:4058–67 [PubMed: 22990013]
28. Casey SC, Tong L, Li Y, Do R, Walz S, Fitzgerald KN, et al. MYC regulates the antitumor immune response through CD47 and PD-L1. Science 2016;352:227–31 [PubMed: 26966191]
29. Shimura T, Takenaka Y, Tsutsumi S, Hogan V, Kikuchi A, Raz A. Galectin-3, a novel binding partner of beta-catenin. Cancer Res 2004;64:6363–7 [PubMed: 15374939]

30. Shimura T, Takenaka Y, Fukumori T, Tsutsumi S, Okada K, Hogan V, et al. Implication of galectin-3 in Wnt signaling. Cancer Res 2005;65:3535–7 [PubMed: 15867344]
31. Erratum for the Report “MYC regulates the antitumor immune response through CD47 and PD-L1” by Casey SC, Tong L, Li Y, Do R, Walz S, Fitzgerald KN, Gouw AM, Baylot V, Gutgemann I, Eilers M, Felsher DW Science 2016;352
32. Muller E, Speth M, Christopoulos PF, Lunde A, Avdagic A, Oynebraten I, et al. Both Type I and Type II Interferons Can Activate Antitumor M1 Macrophages When Combined With TLR Stimulation. Front Immunol 2018;9:2520 [PubMed: 30450098]
33. King KR, Aguirre AD, Ye YX, Sun Y, Roh JD, Ng RP Jr., et al. IRF3 and type I interferons fuel a fatal response to myocardial infarction. Nat Med 2017;23:1481–7 [PubMed: 29106401]
34. Krausgruber T, Blazek K, Smallie T, Alzabin S, Lockstone H, Sahgal N, et al. IRF5 promotes inflammatory macrophage polarization and TH1-TH17 responses. Nat Immunol 2011;12:231–8 [PubMed: 21240265]
35. Steinberg C, Eisenacher K, Gross O, Reindl W, Schmitz F, Ruland J, et al. The IFN regulatory factor 7-dependent type I IFN response is not essential for early resistance against murine cytomegalovirus infection. Eur J Immunol 2009;39:1007–18 [PubMed: 19283778]
36. Woo SR, Fuertes MB, Corrales L, Spranger S, Furdyna MJ, Leung MY, et al. STING-dependent cytosolic DNA sensing mediates innate immune recognition of immunogenic tumors. Immunity 2014;41:830–42 [PubMed: 25517615]
37. Theruvath J, Menard M, Smith BAH, Linde MH, Coles GL, Dalton GN, et al. Anti-GD2 synergizes with CD47 blockade to mediate tumor eradication. Nat Med 2022;28:333–44 [PubMed: 35027753]
38. Jiang Z, Sun H, Yu J, Tian W, Song Y. Targeting CD47 for cancer immunotherapy. J Hematol Oncol 2021;14:180 [PubMed: 34717705]
39. Liu J, Wang L, Zhao F, Tseng S, Narayanan C, Shura L, et al. Pre-Clinical Development of a Humanized Anti-CD47 Antibody with Anti-Cancer Therapeutic Potential. PLoS One 2015;10:e0137345 [PubMed: 26390038]
40. Barkal AA, Weiskopf K, Kao KS, Gordon SR, Rosental B, Yiu YY, et al. Engagement of MHC class I by the inhibitory receptor LILRB1 suppresses macrophages and is a target of cancer immunotherapy. Nat Immunol 2018;19:76–84 [PubMed: 29180808]
41. Manguso RT, Pope HW, Zimmer MD, Brown FD, Yates KB, Miller BC, et al. In vivo CRISPR screening identifies Ptpn2 as a cancer immunotherapy target. Nature 2017;547:413–8 [PubMed: 28723893]
42. Liu X, Pu Y, Cron K, Deng L, Kline J, Frazier WA, et al. CD47 blockade triggers T cell-mediated destruction of immunogenic tumors. Nat Med 2015;21:1209–15 [PubMed: 26322579]
43. Willingham SB, Volkmer JP, Gentles AJ, Sahoo D, Dalerba P, Mitra SS, et al. The CD47-signal regulatory protein alpha (SIRPa) interaction is a therapeutic target for human solid tumors. Proc Natl Acad Sci U S A 2012;109:6662–7 [PubMed: 22451913]
44. Weiskopf K, Ring AM, Ho CC, Volkmer JP, Levin AM, Volkmer AK, et al. Engineered SIRPalpha variants as immunotherapeutic adjuvants to anticancer antibodies. Science 2013;341:88–91 [PubMed: 23722425]
45. Tao H, Qian P, Wang F, Yu H, Guo Y. Targeting CD47 Enhances the Efficacy of Anti-PD-1 and CTLA-4 in an Esophageal Squamous Cell Cancer Preclinical Model. Oncol Res 2017;25:1579–87 [PubMed: 28337964]
46. Chao MP, Alizadeh AA, Tang C, Myklebust JH, Varghese B, Gill S, et al. Anti-CD47 antibody synergizes with rituximab to promote phagocytosis and eradicate non-Hodgkin lymphoma. Cell 2010;142:699–713 [PubMed: 20813259]
47. Wang R, Song S, Harada K, Ghazanfari Amlashi F, Badgwell B, Pizzi MP, et al. Multiplex profiling of peritoneal metastases from gastric adenocarcinoma identified novel targets and molecular subtypes that predict treatment response. Gut 2020;69:18–31 [PubMed: 31171626]
48. Miyazaki J, Hokari R, Kato S, Tsuzuki Y, Kawaguchi A, Nagao S, et al. Increased expression of galectin-3 in primary gastric cancer and the metastatic lymph nodes. Oncology reports 2002;9:1307–12 [PubMed: 12375039]

49. Dong WG, Yu QF, Xu Y, Fan LF. Li-cadherin is inversely correlated with galectin-3 expression in gastric cancer. Digestive diseases and sciences 2008;53:1811–7 [PubMed: 17999183]

50. Kim SJ, Lee HW, Gu Kang H, La SH, Choi IJ, Ro JY, et al. Ablation of galectin-3 induces p27(KIP1)-dependent premature senescence without oncogenic stress. Cell death and differentiation 2014;21:1769–79 [PubMed: 24971481]

Significance:

Dual inhibition of CD47 and Gal-3 enhances tumor cell phagocytosis and reprograms macrophages to overcome the immunosuppressive microenvironment and suppress tumor growth in peritoneal metastasis of gastric adenocarcinoma.

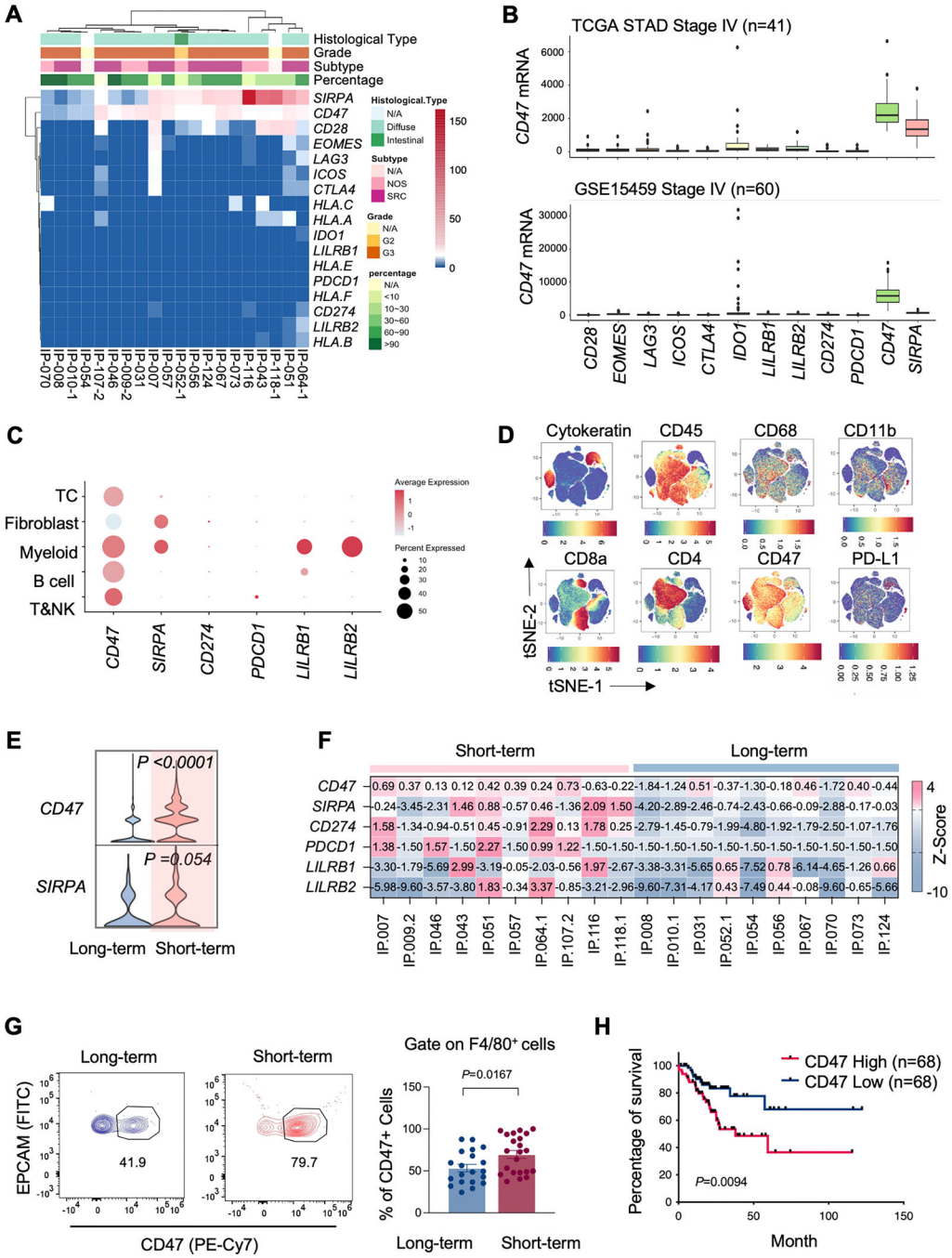

Figure 1. "Do not eat me" gene CD47 is enriched in peritoneal metastases of GAC and associated with poor survival.

A, Bulk RNA-seq analysis on PC specimen (n = 20) using a curated panel of immune checkpoint and "don't eat me" gene. Unsupervised hierarchical clustering was performed on the normalized RNA expression data of indicated genes. **B,** Box plot analysis showed immune checkpoint and "don't eat me" genes of stage IV of TCGA STAD (n=41) and GSE15459 (n=60). **C,** Expression profile of "don't eat me" genes *CD47*, *SIRPA*, *CD274, PDCD1, LILRB1 and LILRB2* were shown in dot-plot with normalized expression levels

of indicated genes from scRNA-seq data. **D,** CD47 and PD-L1 were detected on 6 representative PC ascites samples, as examined by CyTOF using antibodies against notable cell type markers, and CD47 and PD-L1. **E,** Normalized expression levels of *CD47* and *SIRPA* in tumor cluster and myeloid cluster between long-term survivors and short-term survivors was shown as violin plots (P<0.0001). **F,** "Don't eat me" genes *CD47*, *SIRPA*, *CD274, PDCD1, LILRB1 and LILRB2* were shown on the heatmap based on bulk RNA-seq analysis on PCs patients with long-term survivors (>12 month) and short-term survivors (<8 month). **G,** Representative contour plots (left) and quantification of CD47 expression (right) on $EpCAM^+$ tumor cells detected on PC samples between long-term survivor (>12 month) and short-term survivor (<8 month) (n=42), as assessed by flow cytometry. **H,** The association of *CD47* and overall survival of complete responders (CR) patients from TCGA dataset (n=136). Log rank (Mantel-Cox) test was used.

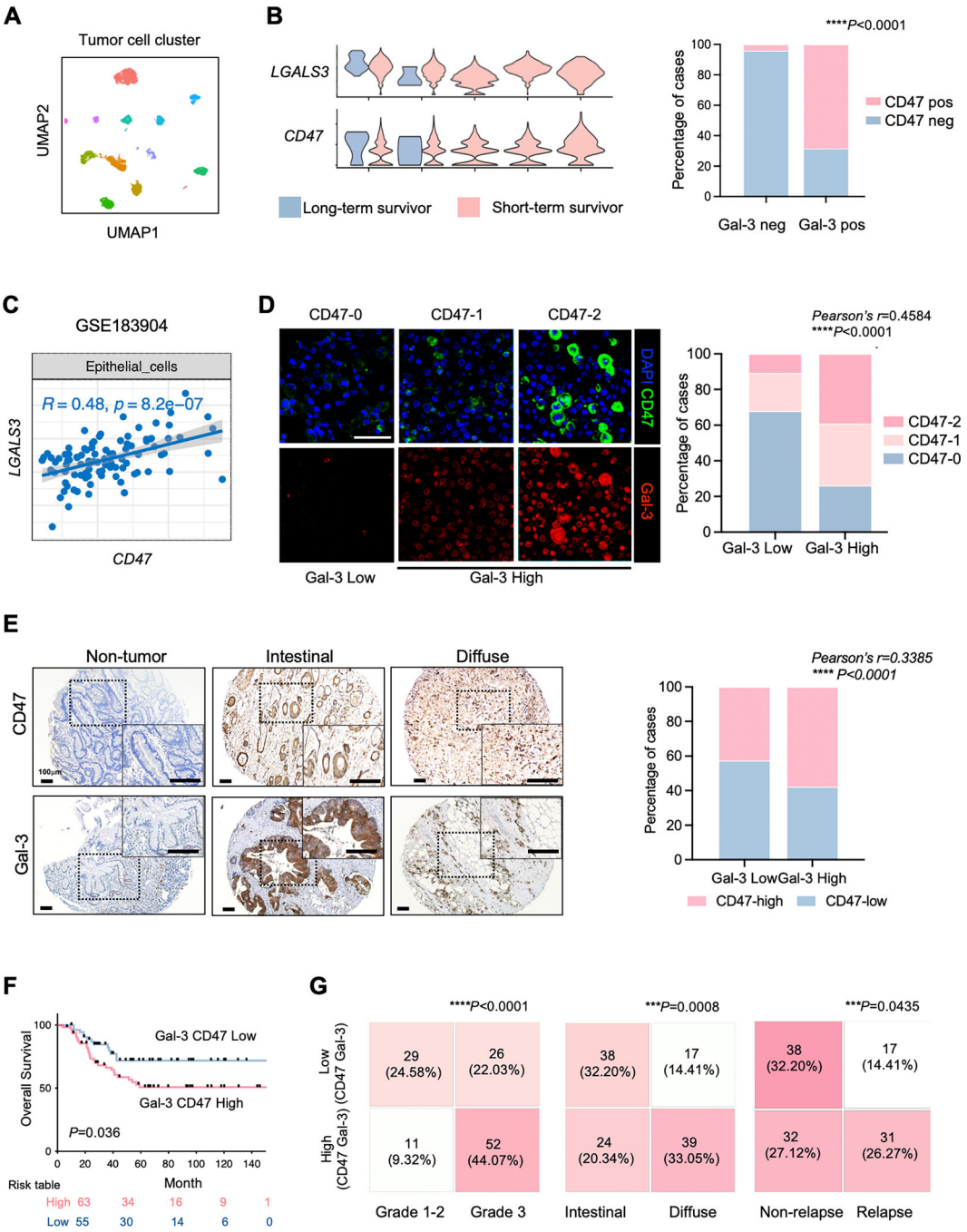

Figure 2. CD47 overexpression corelated with Gal-3 in PC specimens of GAC.

A, scRNA-seq analysis of unfractionated tumor cells from 20 PC samples. **B**, Normalized expression levels of *LGALS3* and *CD47* in tumor cell clusters between long-term survivors and short-term survivors is shown by violin plots (left). Correlation between *LGALS3* and *CD47* in short-term survivor tumor clusters from scRNA-seq data (P<0.0001, right). **C,** Scatter plot showed the correlation of *LGALS3* and *CD47* in epithelial cells in GEO183904 cohort. **D,** Representative immunofluorescence images (left) and the association analysis (right) of Gal-3 and CD47 staining on PC samples (n=51). Scale bar: 50 μm. **E,**

Representative immunohistology staining of Gal-3 and CD47 images of intestinal and diffuse type in TMA samples (left). Scale bar: 100 μm. The association analysis of Gal-3 and CD47 staining in primary GAC of TMA (n=210; $P<0.0001$, right). **F,** The association of Gal-3 and CD47 high expression and low expression with overall survival in TMA samples. **G,** The association of CD47 and Gal-3 high expression with tumor grade ($P<0.0001$), diffuse type ($P=0.0008$) and tumor relapse ($P=0.0435$) respectively. Student's test was used unless otherwise indicated.

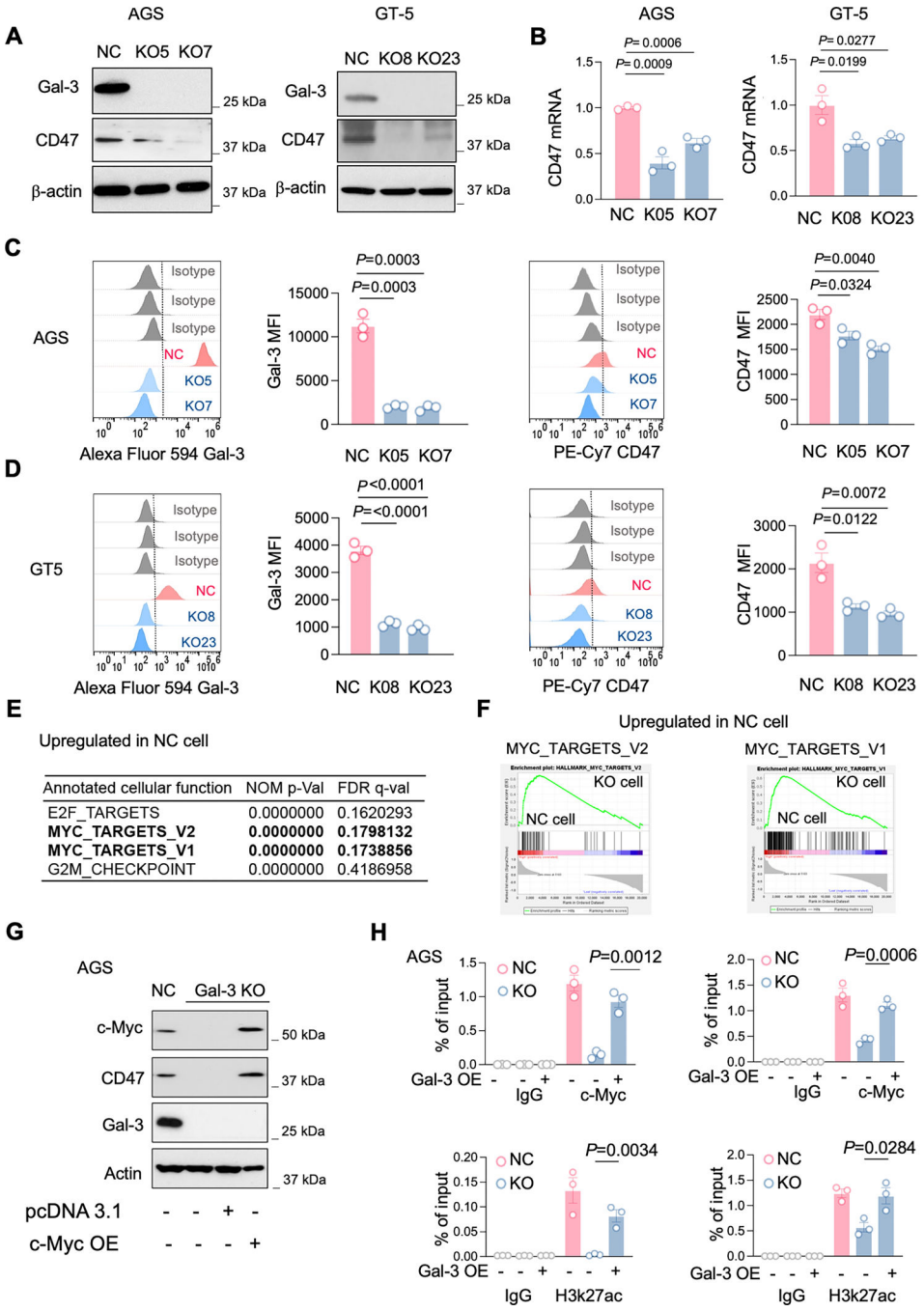

Figure 3. Depletion of Gal-3 suppressed CD47 expression in GAC cells.

A, Western blot analysis of Gal-3 and CD47 expression in AGS and GT5 cells with or without Gal-3 KO (n = 3 biological replicates). **B,** The expression levels of *CD47* mRNA examined by qRT-PCR in NC and Gal-3 KO cells in both AGS and GT5 cells (n = 3 biological replicates). **C and D,** Representative histogram level and quantification of Gal-3 and CD47 in NC and Gal-3 KO cells in AGS and GT5 cells by flow cytometry, respectively (n = 3 biological replicates). **E and F,** Highly upregulated hallmark pathways were revealed by GSEA analysis of RNAseq data in AGS NC cells compared with Gal-3 KO cells. **G,**

The expression level of c-Myc, CD47 and Gal-3 was determined by Western blot (n = 3 biological replicates) in Gal-3 KO AGS cells with or without overexpression of c-Myc. **H**, Quantitative ChIP-qPCR analysis was performed using CD47 promoter primers spanning c-Myc binding site after chromatin pulldown using c-Myc and H3k27ac antibodies in AGS Gal-3 KO cells with or without rescued Gal-3 overexpression (n = 3 biological replicates). Student's test was used unless otherwise indicated.

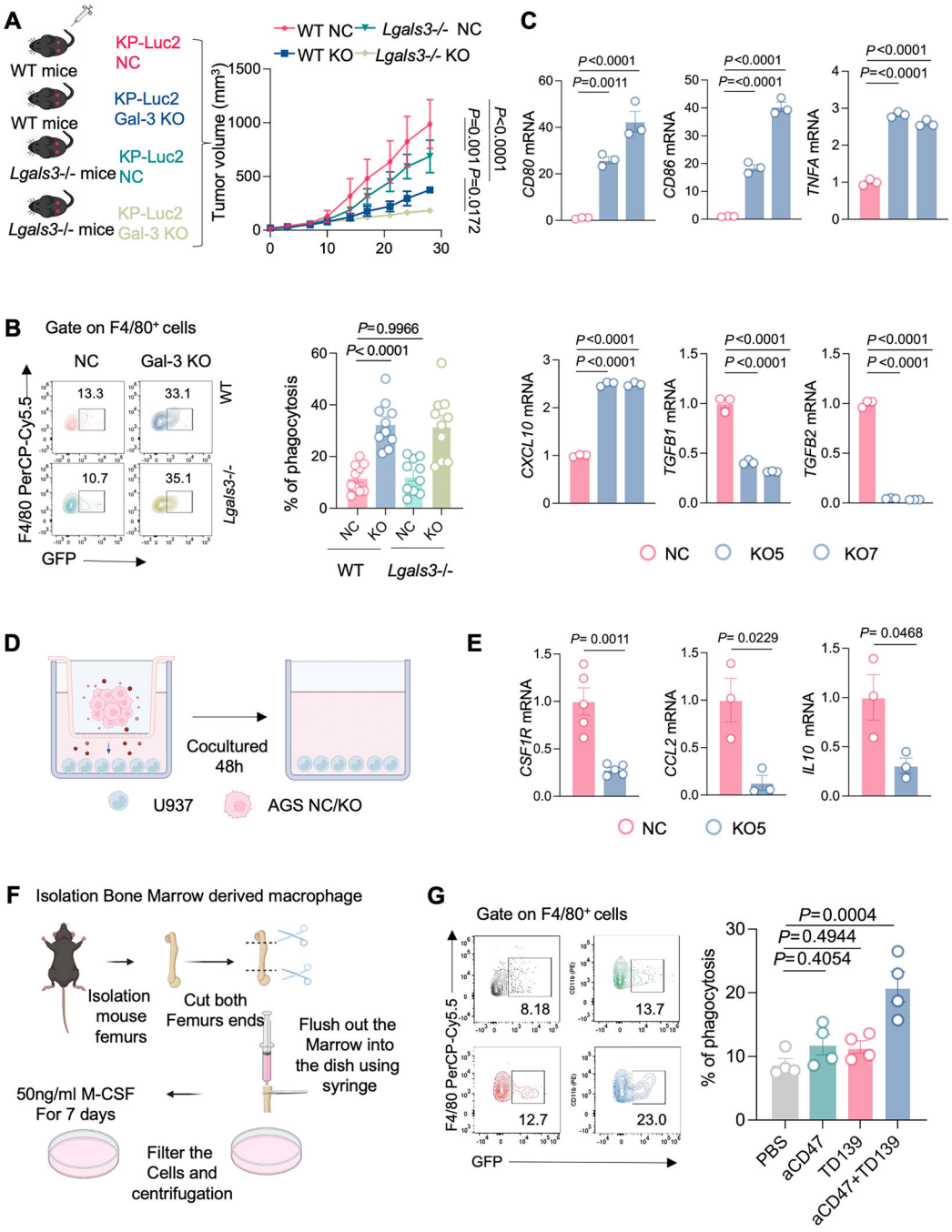

Figure 4. Depletion of Gal-3 promotes phagocytosis by repolarizing macrophages.

A, Diagram of inoculation of KP-Luc2 NC and Gal-3 KO cells in C57BL/6 WT and *Lgals3* KO mice (left). Tumor growth engrafted with KP-Luc2 NC and Gal-3 KO cells in both C57BL/6 WT and *Lgals3* KO mice were measured (n = 5mice per group, right). **B**, Representative contour plots and quantification phagocytosis of KP-Luc2 NC and Gal-3 KO cells in both C57BL/6 WT and *Lgals3* KO mice at the end point of experiment by flowcytometry.

C, Expression levels of *CD80, CD86, TNF* (upper), *CXCL10, TGFB1* and *TGBF2* (bottom) were examined qRT-PCR in primary human donor-derived macrophages co-cultured with NC and Gal-3 KO cells of AGS for 48h (n = 3 biological replicates). **D**, Diagram of Diagram demonstrates the experiments procedure of co culturing U937 with AGS NC and AGS Gal-3 KO cell. **E**, U937 was treated with 80nM PMA for 48h, and co-cultured with NC and Gal-3 KO cells of AGS for 48h, expression levels of *CSF1, CCL2 and IL10* were examined by qRT-PCR (n = 3 biological replicates). **F**, Diagram demonstrates the isolation of macrophage from bone marrow of mice. **G,** Representative contour plots and quantification of phagocytosis of KP-Luc2 by BMDMs pretreated with αCD47, TD139 and combination treatment for 48 h (n = 4/group), as examined by flow cytometry. One-way ANOVA was used in A, B, G. Student's test was used unless otherwise indicated.

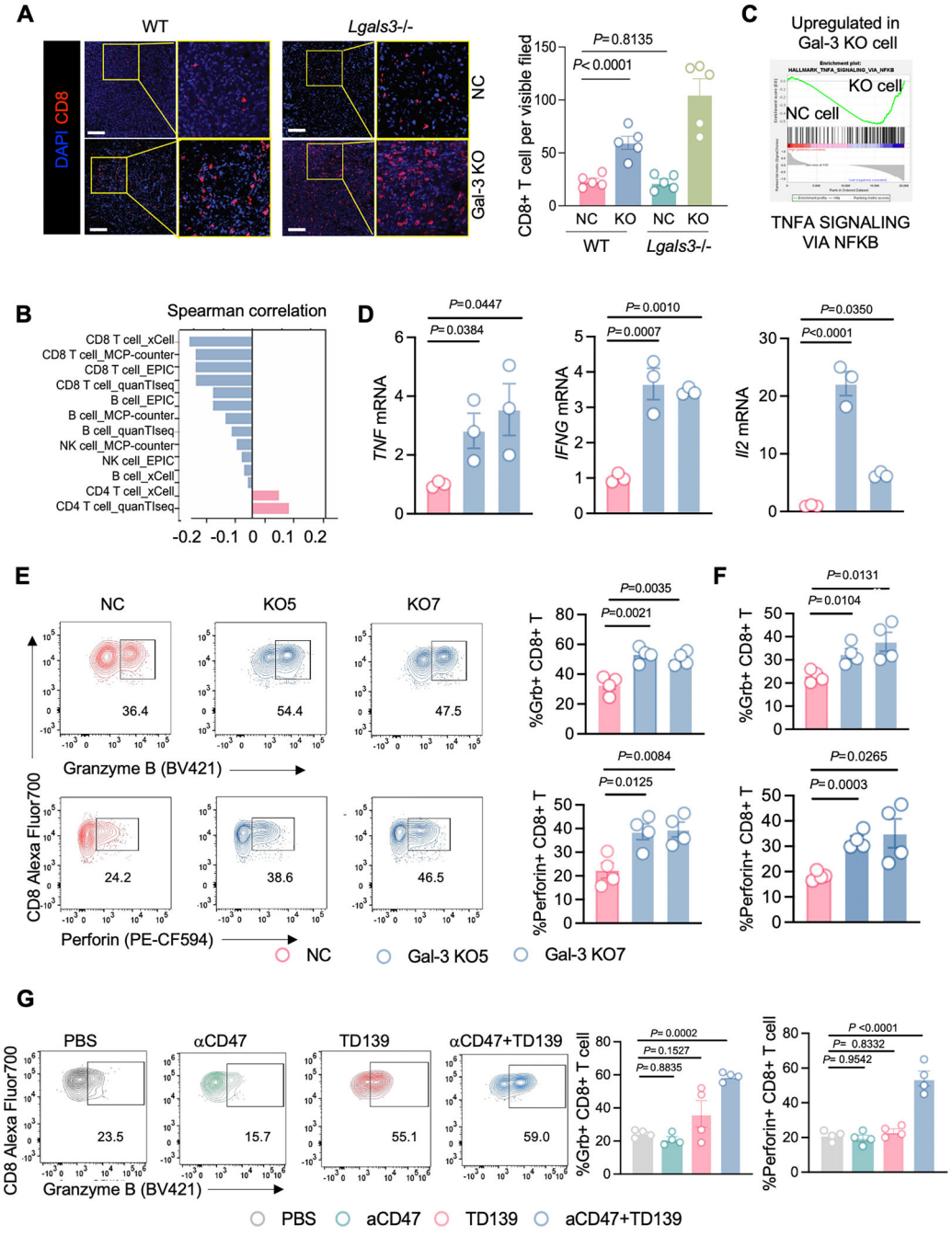

Figure 5. Inhibition of Gal-3 boosted T cell responses in GAC.

A, Representative immunofluorescence staining images (left) and quantification (right) of $CD8^+$ in KP-Luc2 NC and Gal-3 KO cells in WT and *Lgals3*−/− KO mice (n = 5 mice per group). Scale bars, 50 μm. **B,** Spearman correlation of *LGALS3* expression and $CD8^+$ T cell, $CD4^+$ T cell, B cell and NK cell infiltration by MCP-counter, quaTIseq and xCELL algorithm in TCGA STAD cohort (n=415). **C**, Highly upregulated hallmark pathways were revealed by GSEA analysis of RNAseq data in AGS Gal-3 KO cells compared with NC cells. **D**, The expression levels of *TNF, IL2* and *IFNG* examined by qRT-PCR in

human PBMCs co-cultured with AGS NC and Gal-3 KO cells for 48h (n = 3/group). **E,** Representative contour plots and quantification of GrB and Perforin in $CD8^+$ T cells after co-cultured with of AGS Gal-3 KO or NC cells with CD8 T cells for 48h (n = 4/group), as examined by flow cytometry. **F**, Quantification of GrB and Perforin $CD8^+$ T cells after co-cultured with of GT5 Gal-3 KO or NC cells for 48h (n = 4/group), as examined by flow cytometry. **G**, Representative contour plots (left) and quantification of GrB and Perforin expression (right) in human peripheral $CD8^+$ T cells co-cultured with AGS cells of the indicated treatment (n = 4/group), as examined by flow cytometry. AGS cells was treated with αCD47, TD139 and combination treatment for 48 h before co-culture with PBMCs. One-way ANOVA was used A and G. Student's test was used unless otherwise indicated.

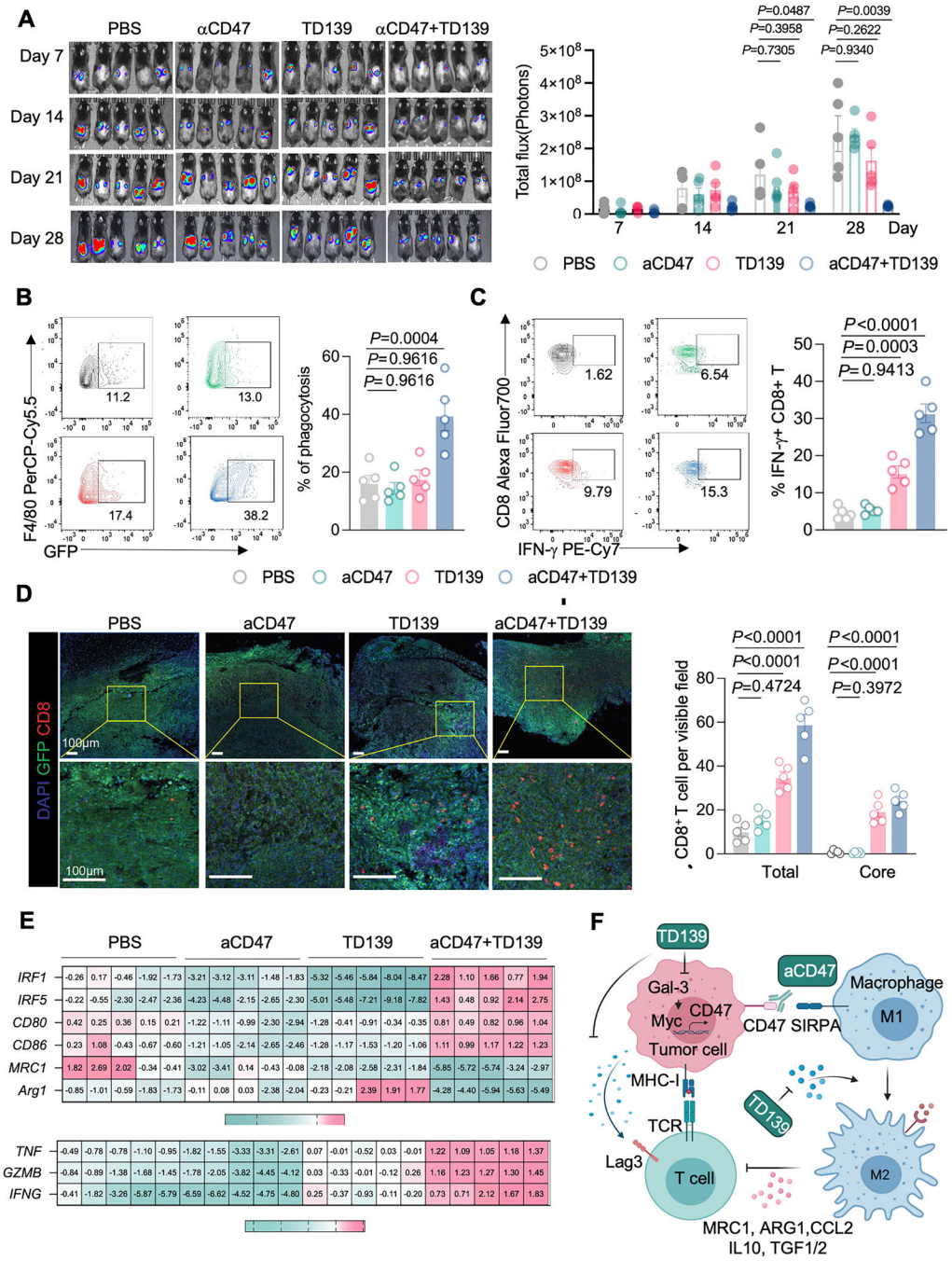

Figure 6. Dual inhibition of Gal-3 and CD47 suppressed tumor growth through increasing phagocytosis and T cell infiltration and response.

A, Representative bioluminescence images over 28 days (left) and quantification (right) of engrafted with KP-Luc2 cell in C57BL/6 mice (n = 5 mice per group) in the indicated treatment. **B**, Representative contour plots and quantification of phagocytosis at the endpoint day 28 (n =5 mice per group), as examined by flow cytometry. **C**, Representative contour plots and quantification of tumor IFNγ^{+}CD8^{+} T cells (n =5 mice per group), as examined by flow cytometry at day 14 (n=5 mice per group). **D**, Representative immunofluorescence

staining images (left) and quantification (right) of tumor infiltrating $CD8^+$ T cells in tumor core and total area (n =5 mice per group). Scale bars, 100 μm. **E**, Notable markers of M1 and M2 Macrophage (top) and T cell related genes expression (bottom) were shown in heatmap of indicated treatment (n=5 mice per group). **F**, Schematic illustration of the impact of Gal-3 and CD47 in phagocytosis and immune regulation in GAC in TME; and co-targeting Gal-3 using TD139 and CD47 using αCD47 antibody synergistically boost both innate and adaptive immune responses that lead to tumor suppression. One-way ANOVA was used A-D.